Journal of Dental Sciences 20 (2025) 1605–1614

Available online at www.sciencedirect.com

ScienceDirect

journal homepage: www.e-jds.com

Original Article

The cell-fate decision of dental follicle stem cells (DFSCs) with porcine corneal extracellular matrix (ECM)

Kuan-Ming Lin [a], Yong-Ren Chen [b,c,d], Ming-Hua Ho [e], Chung-Hsing Li [a,f,g*]

[a] *Graduate Institute of Dental Science, National Defense Medical Center, Taipei, Taiwan*
[b] *Non-invasive Cancer Therapy Research Institute - Taiwan, Taipei, Taiwan*
[c] *Division of Neurosurgery, Department of Surgery, National Taiwan University Hospital, Taipei, Taiwan*
[d] *Graduate Institute of Medical Sciences, National Defense Medical Center, Taipei, Taiwan*
[e] *Department of Chemical Engineering, National Taiwan University of Science and Technology, Taipei, Taiwan*
[f] *Division of Orthodontics, Pediatric Dentistry, and Special Needs Dentistry, Department of Dentistry, Tri-Service General Hospital, Taipei, Taiwan*
[g] *School of Dentistry, National Defense Medical Center, Taipei, Taiwan*

Received 11 December 2024; Final revision received 19 February 2025
Available online 6 March 2025

KEYWORDS
Dental follicle stem cells;
Supercritical carbon dioxide;
Extracellular matrix;
Corneal diseases;
Tissue engineering

Abstract *Background/purpose:* Extracellular matrix (ECM) may be useful as a natural scaffold for tissue engineering. Since dental follicle stem cells (DFSCs) share a similar embryonic origin with corneal keratocytes and endothelial cells and possess the ability to proliferate and differentiate, in this study, we investigate the potential of DFSCs to differentiate into corneal cells under the supercritical carbon dioxide ($SC-CO_2$) decellularized porcine corneal ECM culture stimulation.
Materials and methods: DFSCs were seeded onto the $SC-CO_2$ decellularized porcine corneal ECM and the surrounding culture dish for 21 days. Cell morphology, reverse transcription-quantitative polymerase chain reaction (RT-qPCR), and immunofluorescence staining were used to evaluate the potential of DFSCs to differentiate into corneal epithelial, keratocyte, or endothelial cells. The culture medium was collected every 3 days for growth factor analysis.
Results: The DFSCs cultured on the ECM exhibit notable cell-ECM adhesion and the potential to primarily differentiate into keratocytes, with a partial capacity for differentiation into corneal endothelial cells, while the cells outside the ECM are weakly affected. Growth factor array analysis revealed changes in growth factor expression in different culture conditions, DFSCs, ECM, and DFSCs/ECM co-culture at various time points, indicating a dynamic shift in the

* Corresponding author. School of Dentistry and Graduate Institute of Dental Science, National Defense Medical Center, No. 161, Sec. 6, Minquan E. Rd., Neihu Dist., Taipei City, 11490, Taiwan.
E-mail addresses: chiyenchli@yahoo.com.tw, chiyenchli@mail.ndmctsgh.edu.tw (C.-H. Li).

https://doi.org/10.1016/j.jds.2025.02.019

microenvironment.
Conclusion: The present study demonstrated that DFSCs cultured on the porcine corneal ECM can differentiate mainly into keratocytes-like and partially into corneal endothelial-like cells, exhibiting strong cell-ECM adhesion and regulation of growth factors. Provide insights into the therapeutic application potential of dental-derived stem cells and SC-CO_2 decellularized tissue for corneal diseases.

Introduction

Corneal disease is one of the leading causes of blindness, affecting around 8 million population worldwide.[1] The primary treatment modality for corneal diseases remains corneal transplantation. However, the supply of donor corneas has been insufficient to meet the demand. According to Gain et al., the worldwide average availability is only 1 donor cornea per 70 patients in need.[2] Due to the severe global shortage of donated corneas, research on corneal regeneration, such as gene therapy, stem cell therapy, and tissue engineering has developed.

The dental follicle is a connective tissue derived from the neural crest and formed by ectomesenchymal progenitor cells during the cap stage.[3] In 2004, Morsczeck et al. isolated cells from dental follicles of the human third molar, these cells expressed undifferentiated markers Notch-1 and Nestin and could be maintained in culture for at least 15 passages.[4] Compared to other dental-derived mesenchymal stem cells (MSCs), DFSCs have superior proliferation ability, multipotency, and immunosuppressive effects,[5,6] making them more advantageous for tissue engineering.

In addition to a suitable cell source, tissue architecture plays a crucial role in engineering tissue equivalents. Decellularization refers to the process of removing cellular components from tissues while preserving the ECM components and architecture. The resulting decellularized ECM can serve as a natural bioactive scaffold offering microenvironments known as niches for cells, which can regulate various cellular behaviors, including migration, adhesion, proliferation, and differentiation.[7–9] Previous studies have demonstrated that the composition and topography of the corneal ECM can significantly affect cell behavior. For example, the interaction of corneal endothelial cells with various ECM proteins, such as collagen, fibronectin, and laminin, can enhance cell adhesion, proliferation, and phenotype maintenance,[10] and the aligned nanofiber meshes can promote cell orientation and migration in corneal stromal models.[11] In the field of generating corneal substitutes, decellularized porcine cornea is one of the prominent options of natural scaffold materials since its structure and morphology closely resemble the human cornea, exhibiting similar tissue characteristics and physiological functions.[12,13] And it has also been demonstrated that both human and porcine corneas can be effectively decellularized while maintaining similar patterns of collagen fibrils and glycosaminoglycans preservation.[14]

The SC-CO_2 decellularization technique processes through the high pressure of the fluid to disrupt the cells and then removes the cellular components from the tissue by rapid depressurization.[15] It may serves as an effective alternative to conventional chemical decellularization methods, as it eliminates the risk of cytotoxicity and minimizes damage to the ECM architecture, which are commonly associated with chemical detergent-based methods. SC-CO_2 decellularization has been applied to various tissues, including the aorta and cornea.[15] It has also been demonstrated that SC-CO_2 can effectively remove porcine corneal cells while maintaining the stromal structures and mechanical properties. Furthermore, the scaffold exhibits good biocompatibility and stability after transplantation.[16]

Since DFSCs share a similar embryonic origin with corneal keratocytes and endothelial cells, they may possess inherent advantages for corneal tissue engineering. In this study, we investigate the potential of DFSCs to differentiate into corneal cells under the SC-CO_2 decellularized porcine corneal ECM culture stimulation.

Materials and methods

Cell isolation and culture

The study source of dental follicle tissue is the supernumerary tooth of the patient at the Dentistry Department of Tri-Service General Hospital and was approved by the Tri-Service General Hospital Institutional Review Board (No. C202105066). The tissue was thoroughly minced and washed with phosphate-buffered saline (PBS) (Gibco, Waltham, MA, USA). After centrifuge and discarding the supernatant, dental follicular cells were resuspended in the culture medium (Minimum Essential Medium alpha [MEM α] [Gibco] supplemented with 10 % Fetal Bovine Serum [FBS] [Gibco]), cultured in a 3.5-cm dish and maintained in a humidified environment at 37 °C, 5 % (vol/vol) CO_2 incubator. The medium was replaced when cell attachment was observed. Cells were passaged at 80 % confluence using trypsin and passages 4—10 were used in the present study.

MSCs stemness confirmation

Dental follicular cells (3×10^6) were harvested for flow cytometry. Cells were fixed with 4 % formaldehyde for 15 min at room temperature and then centrifuged with

subsequent PBS washing. Suspend cells in 0.5 % bovine serum albumin (BSA) (Gibco) with antibodies of MSCs positive cell surface cluster of differentiation (CD) markers CD44, CD73, and CD90, and negative markers CD31 (Invitrogen, Waltham, MA, USA), CD34 (TONBO Biosciences, San Diego, CA, USA), and CD45 (Invitrogen) for 1 h at room temperature. Flow cytometer BD FACSCalibur and CellQuest software (BD Biosciences, San Jose, CA, USA) were used for data acquisition and analysis.

DFSCs-ECM culture stimulation

The SC-CO_2 decellularized porcine corneal matrix (ACRO Biomedical, Kaohsiung, Taiwan) was immersed in the culture medium (MEM α [Gibco] supplemented with 10 % FBS [Gibco]) for 24 h before cell seeding. DFSCs were seeded at a density of 500 cells/cm^2 into three groups: (1) control cells group, in which DFSCs were seeded on the culture dish without matrix, (2) ECM cells group, in which DFSCs were seeded directly on the matrix, and (3) dish cells group which DFSCs were culture on the dish outside the matrix. The medium was collected and replaced every 3 days over a culture period of 21 days.

Live cell fluorescent staining and observation

Remove the culture medium (MEM α [Gibco] supplemented with 10 % FBS [Gibco]) of the ECM cells group and rehydrated-ECM group, which ECM was rehydrated with culture medium without cell seeding, with subsequent incubation of CellTracker fluorescent probe solution (Invitrogen) at 37 °C for 30 min. After removing the CellTracker solution, the culture medium was added to the samples for live cell staining observation under the confocal microscope LSM980 (Carl Zeiss, Jena, Germany).

Scanning electron microscope (SEM) sample preparation

In addition to the ECM cells and rehydrated-ECM group, a third group of samples was prepared for SEM observation: the dried-ECM group, which consisted of the original decellularized porcine corneal ECM without rehydration. Briefly, after a culture period of 21 days, the samples were prepared by fixing with a series of glutaraldehyde solutions incubation from 0.5 %, 1.0 %—2.5 %, dehydrating with increased concentrations of ethanol solutions from 30 %, 50 %, 70 %, 80 %, 90 %, 95 %—99 %, and drying in a critical point drier with liquid CO_2. The samples were then mounted, coated with conductive material, and observed under the SEM JSM-7900F (JEOL, Tokyo, Japan).

RT-qPCR

The control, ECM, and dish cells groups were lysed in TRIzol reagent (Invitrogen) and followed the manufacturer's instructions to precipitate, wash, and solubilize the ribonucleic acid (RNA). RNA was quantified using the NanoDrop One Microvolume UV—Vis Spectrophotometer (Thermo Fisher Scientific, Waltham, MA, USA) and then transcribed into complementary deoxyribonucleic acid (cDNA) using Maxima H Minus cDNA Synthesis Master Mix (Thermo Fisher Scientific) with ProFlex PCR System (Applied Biosystems, Waltham, MA, USA) according to the manufacturer's instructions. For PCR reactions, TaqMan Fast Advanced Master Mix (Applied Biosystems) and TaqMan Assays (Thermo Fisher Scientific) were used for the corneal epithelial cell gene cadherin 1 (CDH1) (Hs01023894_m1) and keratin 5 (KRT5) (Hs00361185_m1), keratocyte gene keratocan (KERA) (Hs00559942_m1), and corneal endothelial cell gene sodium/potassium-transporting ATPase subunit alpha-1 (ATP1A1) (Hs00167556_m1) and cadherin 2 (CDH2) (Hs00983056_m1) detection followed the manuscript's instructions. Amplification was performed on QuantStudio 5 Flex Real-Time PCR System (Applied Biosystems). All values were normalized to the endogenous reference gene GAPDH (Hs99999905_m1). Relative quantification of gene expression was performed using the delta—delta cycle threshold ($\Delta\Delta$CT) method.

Immunofluorescence staining

The control, ECM, and dish cells groups were cultured in chamber slides (ibidi GmbH, Martinsried, Germany) and fixed in 4 % formaldehyde at 4 °C for 15 min. After washing with PBS, cells were permeabilized in 0.1 % Triton X-100 for 5 min with subsequent PBS washing. Blocking in 3 % BSA for 30 min with subsequent PBS washing. Samples were incubated overnight at 4 °C with primary antibody solutions of corneal epithelial cell (epithelial cadherin [E-cadherin] and Cytokeratin 5 [CK5]) (Abcam, Cambridge, UK), keratocyte (Keratocan) (Cloud-Clone Corp, Katy, TX, USA), and corneal endothelial cell (sodium/potassium-adenosine triphosphatase [Na^+/K^+-ATPase] and neural cadherin [N-cadherin]) (Abcam). Counterstaining with corresponding fluorescein isothiocyanate (FITC) and allophycocyanin (APC) secondary antibodies (Jackson ImmunoResearch, West Grove, PA, USA) for 1 h at room temperature before counterstaining with 4′,6-diamidino-2-phenylindole (DAPI). The chambers were removed, and the slides were mounted with coverslips before the observation under the THUNDER Imager (Leica Camera, Wetzlar, Germany).

Growth factor array analysis

The original culture medium (MEM α [Gibco] supplemented with 10 % FBS [Gibco]) (control medium) and the culture medium in control cells (DFSCs medium), rehydrated-ECM (ECM medium), and ECM cells group (ECM cells medium) were collected every 3 days for 21 days. Samples were taken on days 1—3, 7—9, and 19—21 for growth factor analysis following the manufacturer's instructions (Human Growth Factor Array C1) (RayBiotech, Peachtree Corners, GA, USA). Briefly, the antibody arrays were blocked with blocking buffer and incubated for 30 min at room temperature. After aspiration, medium samples were added to cover the antibody arrays and incubated for 3 h at room temperature with subsequent wash. Biotinylated antibody cocktails were added to arrays and incubated at 4 °C overnight with subsequent wash. Arrays were incubated with horseradish peroxidase (HRP)-Streptavidin for 2 h at room temperature. After washing, the arrays were covered with chemiluminescence detection buffers and then

captured with the chemiluminescent imaging system (Xplorer) (SPOT Imaging Solutions, Sterling Heights, MI, USA). Growth factor array images were analyzed using the ImageLab software (Bio-Rad Laboratories, Hercules, CA, USA) and RayBio® analysis tools (RayBiotech). A $\geq$1.5-fold difference in growth factor expression between the samples and the control medium was considered a meaningful change in the present study.

Statistical analysis

Statistical analysis was performed using GraphPad Prism version 9 (GraphPad Software Inc., San Diego, CA, USA). Multiple group comparisons were conducted via one-way ANOVA with Tukey's post hoc test. *P*-value less than 0.05 ($P < 0.05$) was considered statistically significant. Data are presented as mean $\pm$ standard error of the mean (SEM), with a sample size of 3 for each group ($n = 3$) with 2 replicates.

Results

Live cell fluorescent staining

Through confocal microscopy and live cell staining on day 21 of culture, we found that the matrix patterns can be faintly observed in both rehydrated ECM and ECM cells groups (Fig. 1A, B, and D). The ECM cells group (Fig. 1B—D) displays cells with fibroblastic morphology and bipolar orientation under the bright field, green emission fluorescence, and a merge of bright field and green fluorescence images, respectively.

SEM observation

SEM was used to observe the morphology and cell attachment of DFSCs on day 21 of SC-CO_2 decellularized porcine corneal ECM culture stimulation. Compared to the yellow H-like symbol in the dried-ECM group, which represents a width of approximately 13 μm (Fig. 2A), the groove-like structure in the rehydrated-ECM group has a width of around 6.5 μm, as indicated by the blue H-like symbol (Fig. 2B), indicating a more swollen and complex topography that emphasizes the three-dimensional structures in rehydrated-ECM. In the ECM cells group (Fig. 2C), it was observed that some cells attached to the ECM display bipolar morphology and grow along the underlying orientation of the matrix as indicated by red dotted-line arrows.

RT-qPCR

Relative quantification of RT-qPCR and one-way ANOVA with Tukey's multiple comparison analysis were used to compare the differentiation of DFSCs on day 21 of SC-CO_2 decellularized porcine corneal ECM culture stimulation (Fig. 3). Among the control cells, dish cells, and ECM cells group, no signal was detected for the corneal epithelial cell genes KRT5 and CDH1. For the keratocyte gene KERA, the relative expression in dish cells was not significantly different from that of control and ECM cells. In contrast, the ECM cells showed a significant increase compared to the control cells,

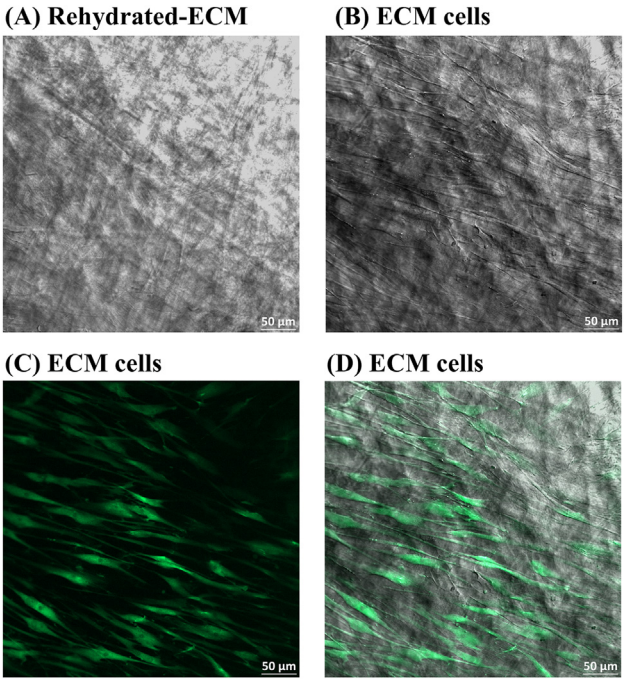

Figure 1 Confocal microscopy observation of rehydrated-extracellular matrix (ECM) and ECM cells with live cell staining on day 21. Rehydrated-ECM represents the rehydrated supercritical carbon dioxide (SC—CO_2) decellularized porcine corneal ECM without cell seeding (A). ECM cells represent the dental follicle stem cells (DFSCs) culture on the SC-CO_2 decellularized porcine corneal ECM under the bright field (B), green emission fluorescence (C), and a merge of bright field and green fluorescence images (D). Scale bars, 50 μm. (For interpretation of the references to colour in this figure legend, the reader is referred to the Web version of this article.)

with a *P*-value of 0.006. For the first corneal endothelial cell gene, ATP1A1, ECM cells had a slightly lower expression than control and dish cells, with *P*-values $<$0.001, while the control and dish cells expressed no significant differences. For the second endothelial gene, CDH2 demonstrated no significant differences among the three groups.

In summary, corneal epithelial cell genes were not detected in any groups, and there were no significant differences in keratocyte and endothelial cell gene expression between control and dish cells. Compared to control cells, ECM cells showed a significant increase in keratocyte gene (KERA) expression and a slight decrease in corneal endothelial cell gene (ATP1A1) expression, with *P*-values less than 0.05.

Immunofluorescence staining

Immunofluorescence staining was used to identify the differentiation status of DFSCs on day 21 of SC-CO_2 decellularized porcine corneal ECM culture stimulation (Fig. 4). In the control cells group (Fig. 4A—D), corneal cells-related marker proteins were not detected. Additionally, the dish cells (Fig. 4E) and ECM cells (Fig. 4I) did not express the corneal epithelial cell markers CK5 and E-cadherin. In

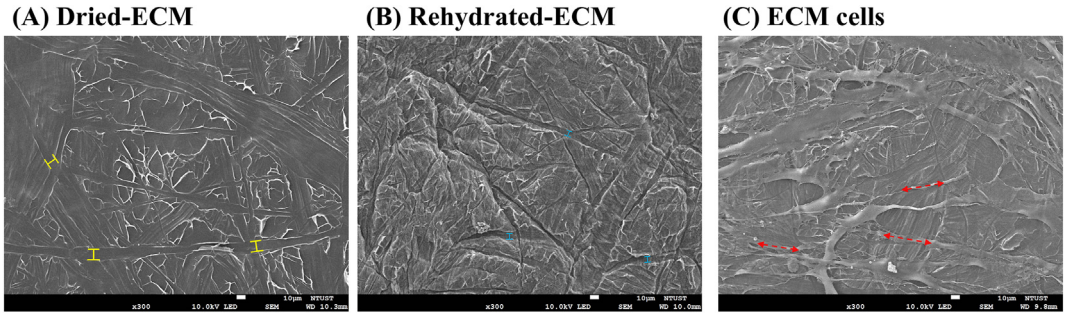

Figure 2 Scanning electron microscope (SEM) observation of dried-extracellular matrix (ECM), rehydrated-ECM, and ECM cells on day 21. Dried-ECM and rehydrated-ECM represent the dried and rehydrated supercritical carbon dioxide (SC–CO_2) decellularized porcine corneal ECM without cell seeding (A and B). ECM cells represent the dental follicle stem cells (DFSCs) cultured on the SC-CO_2 decellularized porcine corneal ECM (C). Yellow and blue H-like symbols indicating the groove-like structure. Red dotted-line arrows indicate the cells following the orientation of ECM. Scale bars, 10 μm. (For interpretation of the references to colour in this figure legend, the reader is referred to the Web version of this article.)

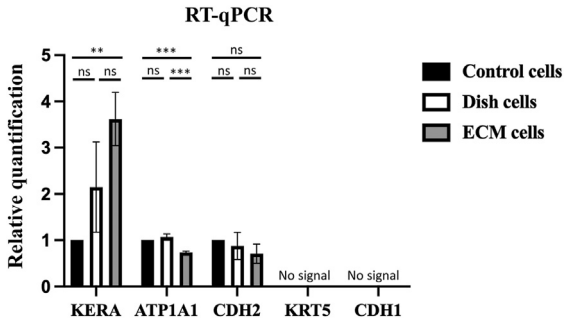

Figure 3 Relative quantification of gene expression by reverse transcription-quantitative polymerase chain reaction (RT-qPCR) on day 21 in control cells, dish cells, and extracellular matrix (ECM) cells groups. Expression of corneal epithelial cell genes (KRT5 and CDH1), keratocyte gene (KERA), and corneal endothelial cell genes (ATP1A1 and CDH2) were analyzed in the control cells, dish cells, and ECM cells group. Results represent mean ± SEM ($n = 3$). *P*-value greater than 0.05 was considered to have **no significance (ns)**. $0.01 < P \leq 0.05$: *. $0.001 < P \leq 0.01$: **. $P \leq 0.001$: ***. Abbreviation: KRT5-keratin 5, CDH1- cadherin 1, KERA-keratocan, ATP1A1-sodium/potassium-transporting ATPase subunit alpha-1, CDH2- cadherin 2.

contrast, the ECM cells exhibited expression of the keratocyte marker Keratocan as well as the corneal endothelial cell markers Na^+/K^+-ATPase and N-cadherin (Fig. 4J–L). Among these, Keratocan demonstrated the strongest fluorescence signal. Interestingly, the dish cells also displayed Keratocan, Na^+/K^+-ATPase, and N-cadherin expression (Fig. 4F–H), but the fluorescence intensity was noticeably weaker compared to the ECM cells group. Furthermore, the positive staining in the dish cells was mostly limited to the cell layers directly adjacent to the ECM border (white dotted line).

Growth factor array analysis

Control medium, DFSCs medium, ECM medium, and ECM cells medium were collected every 3 days for 21 days. Samples were taken on days 1–3, 7–9, and 19–21 for growth factor analysis (Fig. 5). ImageLab software was used to quantify the signal intensities of the chemiluminescent image (Fig. 5A) in accordance with the growth factor profile (Fig. 5B). Since our culture medium (MEM α [Gibco] supplemented with 10 % FBS [Gibco]) is composed of a high concentration of serum, which may contain various growth factors, it is recommended to set an original culture medium sample (control medium) as a reference control. Fig. 5C–E presents the data of growth factors with ≥1.5-fold difference between the samples and the control medium on days 1–3, 7–9, and 19–21, respectively.

As shown in Fig. 5C, during days 1–3, the DFSCs medium exhibited over 1.5-fold increases in amphiregulin (AREG), basic fibroblast growth factor (bFGF), beta-nerve growth factor (bNGF), macrophage colony-stimulating factor (M-CSF), transforming growth factor (TGF) -α and β1, and platelet-derived growth factor receptor alpha (PDGF Rα) compared to the control medium. The ECM medium showed over 1.5-fold increases in AREG, bFGF, bNGF, M-CSF, TGF-α and β1, and PDGF Rα and β compared to the control medium. The ECM cells medium had over 1.5-fold increases in AREG, bFGF, bNGF, granulocyte-macrophage colony-stimulating factor (GM-CSF), and M-CSF compared to the control medium. In Fig. 5D, during days 7–9, the DFSCs medium exhibited over 1.5-fold increases in AREG, bFGF, bNGF, epidermal growth factor (EGF), epidermal growth factor receptor (EGFR), and fibroblast growth factor (FGF)-7 compared to the control medium. The ECM medium showed over 1.5-fold increases in AREG, bFGF, bNGF, EGF, EGFR, FGF-4, FGF-6, and FGF-7. The ECM cells medium had over 1.5-fold increases in vascular endothelial growth factor (VEGF), insulin-like growth factor-binding protein (IGFBP)-6, AREG, bFGF, bNGF, EGF, EGFR, FGF-6, and FGF-7. In Fig. 5E, at days 19–21, the DFSCs medium had over 1.5-fold increases in VEGF, IGFBP-2, IGFBP-3, IGFBP-6, EGFR, and hepatocyte growth factor (HGF) compared to the control medium. The ECM medium showed over 1.5-fold increases in bNGF, EGF, and EGFR. The ECM cells medium had over 1.5-fold increases in VEGF, IGFBP-2, IGFBP-3, IGFBP-6, AREG, bFGF, bNGF, EGF, EGFR, and HGF.

In the comparison across three time points, AREG, bFGF, GM-CSF, M-CSF, PDGF R, and TGF-α and β1 demonstrated increased expression compared to the control medium

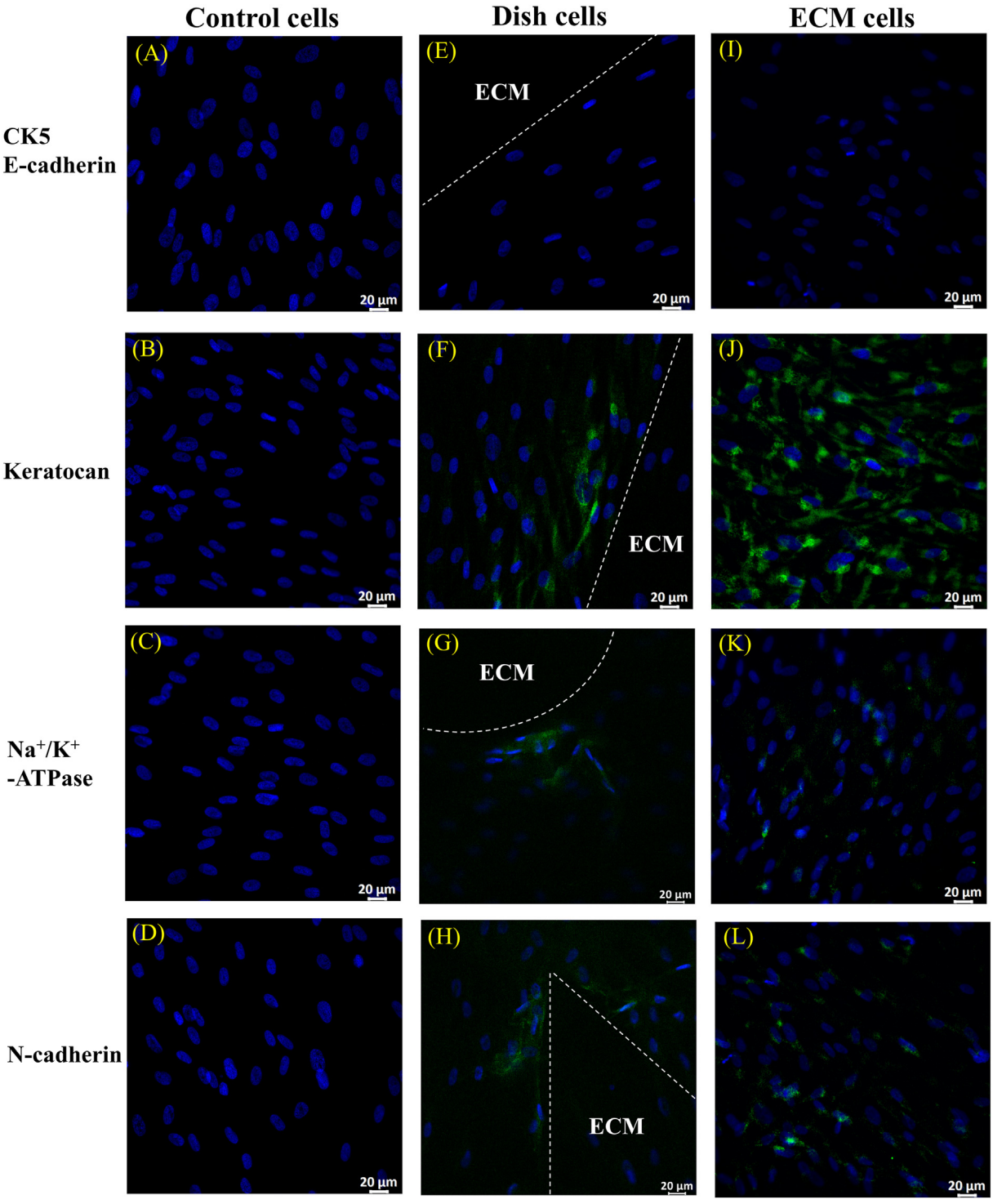

Figure 4 Immunofluorescence staining of dental follicle stem cells (DFSCs) on day 21 of supercritical carbon dioxide ($SC-CO_2$) decellularized porcine corneal extracellular matrix (ECM) culture stimulation. Corneal epithelial cell markers CK5 (green) and E-cadherin (red), keratocyte marker Keratocan (green), and corneal endothelial cell markers Na^+/K^+-ATPase (green) and N-cadherin (green) were used to evaluate corneal differentiation of DFSCs. Control cells represent the DFSCs control group (A–D). Dish cells are the DFSCs cultured on the dish outside the ECM, with white dotted lines representing the border of the matrix (E–H). ECM cells are the DFSCs culture on the ECM (I–L). Scale bars, 20 μm. Abbreviation: CK5- Cytokeratin 5, E-cadherin- epithelial cadherin, Na^+/K^+-ATPase-sodium/potassium-adenosine triphosphatase, N-cadherin- neural cadherin. (For interpretation of the references to colour in this figure legend, the reader is referred to the Web version of this article.)

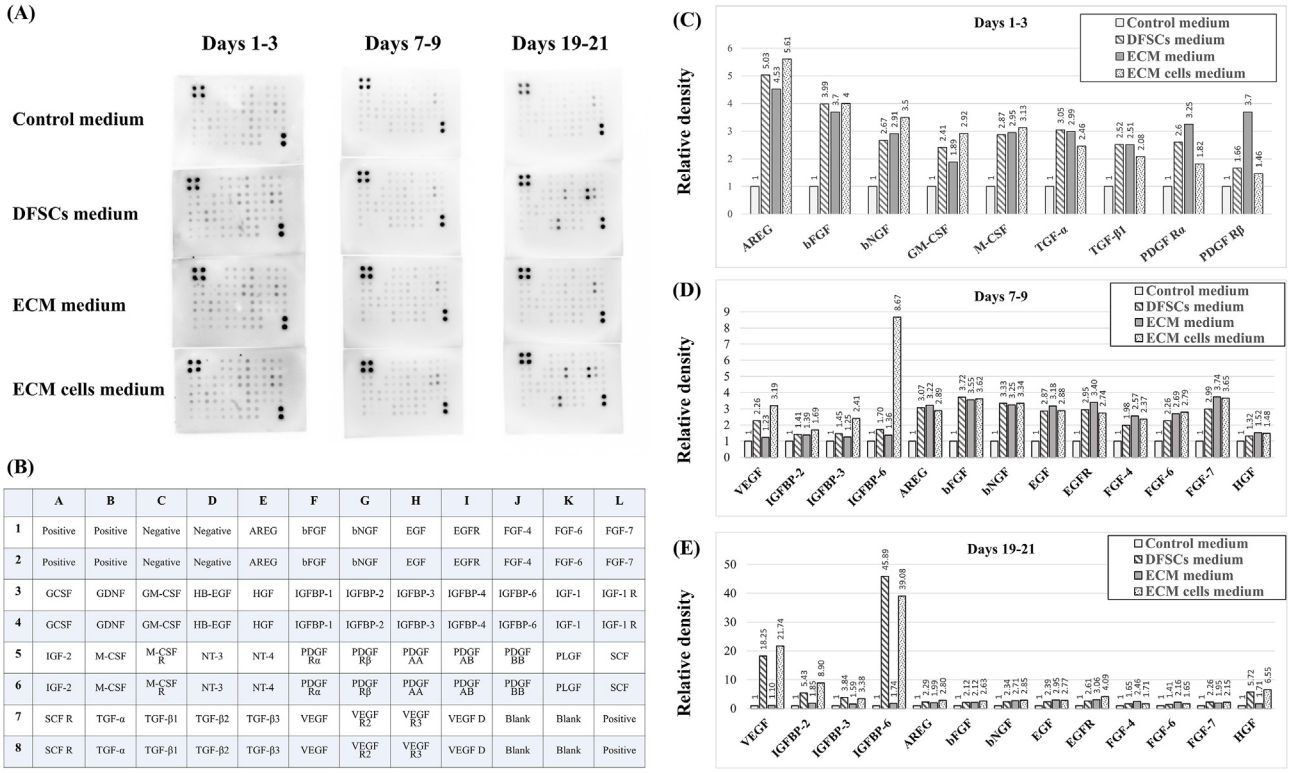

	A	B	C	D	E	F	G	H	I	J	K	L
1	Positive	Positive	Negative	Negative	AREG	bFGF	bNGF	EGF	EGFR	FGF-4	FGF-6	FGF-7
2	Positive	Positive	Negative	Negative	AREG	bFGF	bNGF	EGF	EGFR	FGF-4	FGF-6	FGF-7
3	GCSF	GDNF	GM-CSF	HB-EGF	HGF	IGFBP-1	IGFBP-2	IGFBP-3	IGFBP-4	IGFBP-6	IGF-1	IGF-1 R
4	GCSF	GDNF	GM-CSF	HB-EGF	HGF	IGFBP-1	IGFBP-2	IGFBP-3	IGFBP-4	IGFBP-6	IGF-1	IGF-1 R
5	IGF-2	M-CSF	M-CSF R	NT-3	NT-4	PDGF Rα	PDGF Rβ	PDGF AA	PDGF AB	PDGF BB	PLGF	SCF
6	IGF-2	M-CSF	M-CSF R	NT-3	NT-4	PDGF Rα	PDGF Rβ	PDGF AA	PDGF AB	PDGF BB	PLGF	SCF
7	SCF R	TGF-α	TGF-β1	TGF-β2	TGF-β3	VEGF	VEGF R2	VEGF R3	VEGF D	Blank	Blank	Positive
8	SCF R	TGF-α	TGF-β1	TGF-β2	TGF-β3	VEGF	VEGF R2	VEGF R3	VEGF D	Blank	Blank	Positive

Figure 5 Growth factor array analysis. Chemiluminescent images of the growth factor array for control medium, dental follicle stem cells (DFSCs) medium, extracellular matrix (ECM) medium, and ECM cells medium on days 1—3, 7—9, and 19—21 (A) were analyzed in accordance with the growth factor profile (B). Growth factors with ≥1.5-fold difference compared to the control medium group on days 1—3, 7—9, and 19—21 were presented (C, D, and E). The excluded growth factors are those with a less than 1.5-fold difference compared to the control medium (data not shown). Abbreviation: AREG-amphiregulin, bFGF- basic fibroblast growth factor, bNGF- beta-nerve growth factor, EGF- epidermal growth factor, EGFR-epidermal growth factor receptor, FGF-fibroblast growth factor, GCSF- granulocyte colony-stimulating factor, GDNF- glial cell line-derived neurotrophic factor, GM—CSF— granulocyte-macrophage colony-stimulating factor, HB-EGF- heparin-binding EGF-like growth factor, HGF-hepatocyte growth factor, IGFBP- insulin-like growth factor-binding protein, IGF- insulin-like growth factor, IGF-1R-insulin-like growth factor 1 receptor, M—CSF— macrophage colony-stimulating factor, M-CSF R-macrophage colony-stimulating factor receptor, NT-neurotrophin, PDGF R-platelet-derived growth factor receptor, PDGF- platelet-derived growth factor, PLGF-placenta growth factor, SCF- stem cell factor, SCF R-stem cell factor receptor, TGF- transforming growth factor, VEGF- vascular endothelial growth factor, VEGF R-vascular endothelial growth factor receptor.

during the initial stage. Subsequently, these growth factors showed a declining expression pattern, with some falling below 1.5-fold expression compared to the control medium. The DFSCs medium expressed increasing trends for VEGF, IGFBP-2, IGFBP-3, IGFBP-6, EGF, EGFR, FGF, and HGF in the later stage, while the other factors declined. The ECM medium exhibited decreasing trends of expression in most of the growth factors in the later stage. And the ECM cells medium had increasing trends for VEGF, IGFBP-2, IGFBP-3, IGFBP-6, EGFR, and HGF, while the other factors declined.

Discussion

Previous studies have demonstrated that cells in three-dimensional environments can better access nutrients, oxygen, and signaling molecules.[17,18] In the present study, SEM results revealed that the rehydrated-ECM presented a more complex three-dimensional architecture compared to the dried-ECM, potentially providing a more accurate representation of the *in vivo* cellular microenvironment, and DFSCs also demonstrated successful attachment to the SC-CO_2 decellularized porcine corneal ECM on confocal live cell staining. After 21 days of culture stimulation, SEM observations showed bipolar cells with pseudopodial extensions, similar to the morphological findings reported by Kim et al. when culturing corneal stromal cells on three-dimensional collagen matrices using medium containing 10 % FBS.[19] Furthermore, some cells were found growing along the directional patterns of the underlying matrix structure, which may indicate that the orientation and patterns of ECM may guide the arrangement of the cells. We further performed cell detachment tests by using trypsin and live cell tissue dissociator (*gentleMACS Octo Dissociator* with Heaters) (Miltenyi Biotec, Teterow, Germany). The results demonstrated strong cell-ECM adhesion in which cells were not easily detached in both methods (data not shown). This characteristic may be beneficial for clinical transplantation procedures in the future.

Studies on corneal epithelial regeneration have primarily utilized oral mucosal epithelial cells or MSCs from various tissues.[20–22] However, MSCs typically require specific culture conditions to generate epithelial-like cells through transdifferentiation or mesenchymal–epithelial transition (MET). In the present study, the relative quantification of RT-qPCR and immunofluorescence staining results exhibited that corneal epithelial-related genes (KRT5 and CDH1) and proteins (CK5 and E-cadherin) were not expressed in any groups. Therefore, we suggest that the SC-CO_2 decellularized porcine corneal ECM may lack the necessary molecules to guide the MSC transformation into epithelial cells.

DFSCs cultured on the matrix showed significantly increased expression of the keratocyte-related gene (KERA), while corneal endothelial cell genes (ATP1A1) were slightly decreased. Coupled with the immunofluorescence staining results, the keratocyte protein (Keratocan) exhibited the most intense expression, whereas corneal endothelial cell markers (Na^+/K^+-ATPase and N-cadherin) displayed weak staining, suggesting that SC-CO_2 decellularized porcine corneal ECM microenvironment mainly directing DFSCs differentiation toward a keratocyte phenotype, with a partial capacity for differentiation into corneal endothelial cells.

In contrast, DFSCs attached to the culture dish outside the ECM showed no significant differences in gene expression. The immunofluorescence expressions of Keratocan, Na^+/K^+-ATPase, and N-cadherin are weaker than those of cells cultured on the ECM. Notably, the restricted range of positive staining of the cell layers directly adjacent to the ECM border suggests that the differentiation process may be mediated by short-range paracrine signaling molecules originating from the cell-ECM interaction. This spatial pattern of differentiation may indicate that the influence of SC-CO_2 decellularized porcine corneal ECM on cellular phenotype likely modulates through localized signaling mechanisms rather than long-range effects. These results collectively demonstrate that the ECM provides essential local microenvironmental cues for directing DFSCs differentiation toward a keratocyte lineage.

The interaction between growth factors and the ECM can create a bidirectional regulatory loop that modulates the stability, diffusivity, duration, and intensity of growth factor activity.[23] It has also been illustrated that the interaction between cells and ECM is dynamic reciprocity, which initiates cellular signaling that affects both cell behaviors and ECM composition.[24] The growth factor expression profiles in the present study revealed distinct temporal patterns among different culture conditions.

In the initial stage, the DFSCs, ECM, and ECM medium demonstrated an over 1.5-fold increased expression in AREG, bFGF, and bNGF compared to the control medium. These growth factors are typically associated with cell survival, proliferation, migration, etc.[25–28] However, the detailed mechanism and potential effect of these growth factors on DFSCs and DFSCs-ECM interaction require further investigation. Additionally, the results demonstrated higher expression of GM-CSF and M-CSF in the ECM cells medium, which may indicate a potential immunomodulatory effect during DFSCs-ECM interaction. TGF-α, TGF-β1, and PDGFR play crucial roles in regulating cellular behaviors and ECM dynamics. Previous studies have shown that TGF-a can positively influence cell adhesion,[29] and TGF-β1 can not only modulate the synthesis and deposition of ECM components but also induce corneal fibroblast differentiation into myofibroblasts.[30,31] It is also demonstrated that PDGFR signaling can regulate the collagen gel remodeling.[32] And the relationship between PDGFR and ECM is bidirectional, where PDGFR signaling can affect ECM composition, and conversely, ECM characteristics may regulate PDGFR expression.[33] The present study found that the expression of TGF-α, TGF-β1, PDGF Rα and β were relatively higher in the ECM medium and lower in ECM cells medium, whether these growth factors were activated or consumed during DFSCs-ECM interaction remains an important area for future research.

During days 7–9, DFSCs medium and ECM cells medium demonstrated upregulation of various growth factors, particularly those associated with cell survival, proliferation, migration, etc. (AREG, bFGF, bNGF, EGF, EGFR, and FGF-7). However, bFGF, VEGF, EGF, and other growth factors have also been used or discovered to induce cell differentiation toward keratocytes or affect other behaviors of corneal cells.[34–36] The specific growth factor concentration and related signal pathway to induce DFSCs differentiation toward keratocyte and corneal endothelial cells require further exploration. Moreover, the ECM medium and ECM cells medium showed a broader range of upregulated factors, suggesting that the ECM environment may enhance growth factor productions.

In the later phase (days 19–21), there was a noticeable increase in VEGF, HGF, and IGFBPs in both DFSCs medium and ECM cells medium, which may benefit regenerative medicine by regulating wound healing, angiogenesis, cell survival, etc.[37–39] Notably, ECM can also serve as a local reservoir to sequester or express growth factors to cells.[9] In our study, the ECM medium contains higher levels of growth factors such as AREG, bFGF, bNGF, EGF, EGFR, and FGFs than the control medium, however, the expression levels of these growth factors decreased in days 19–21. This decline may be attributed to alterations in the regulation of growth factors by the ECM or the loss caused by replacing the culture medium. These temporal changes in growth factor expression indicate a dynamic shift in the microenvironment, potentially reflecting different stages of cellular differentiation and matrix remodeling.

In conclusion, our findings demonstrated that DFSCs can effectively adhere to and grow on the decellularized porcine corneal ECM, exhibiting strong cell-ECM attachment. RT-qPCR and immunofluorescence staining revealed that DFSCs cultured on the ECM exhibit a pronounced differentiation potential toward keratocytes and partial capacity toward corneal endothelial cells. Growth factor array analysis exhibited differential expression patterns across various groups and time points, indicating a dynamic shift in the microenvironment. These findings potentially provide insights for advancing corneal tissue engineering and regenerative medicine.

Declaration of competing interest

The authors have no conflicts of interest relevant to this article.

Acknowledgments

We would like to sincerely thank Yu-Chuan Huang, Jian-Liang Chou, and Da-Shin Wang from the Instrument Center of the National Defense Medical Center for their guidance, support, and suggestions throughout this research. The authors gratefully acknowledge the support of Tri-Service General Hospital and the National Taiwan University of Science and Technology by grant TSGH-A-111014 and TSGH-NTUST-111-08.

Appendix A. Supplementary data

Supplementary data to this article can be found online at https://doi.org/10.1016/j.jds.2025.02.019.

References

1. Anitha V, Tandon R, Shah SG, et al. Corneal blindness and eye banking: current strategies and best practices. *Indian J Ophthalmol* 2023;71:3142—8.
2. Gain P, Jullienne R, He Z, et al. Global survey of corneal transplantation and eye banking. *JAMA Ophthalmol* 2016;134:167—73.
3. Sedgley CM, Botero TM. Dental stem cells and their sources. *Dent Clin* 2012;56:549—61.
4. Morsczeck C, Götz W, Schierholz J, et al. Isolation of precursor cells (PCs) from human dental follicle of wisdom teeth. *Matrix Biol* 2005;24:155—65.
5. Zhou T, Pan J, Wu P, et al. Dental follicle cells: roles in development and beyond. *Stem Cells Int* 2019;2019:9159605.
6. Gan L, Liu Y, Cui D, Pan Y, Zheng L, Wan M. Dental tissue-derived human mesenchymal stem cells and their potential in therapeutic application. *Stem Cells Int* 2020;2020:8864572.
7. Theocharis AD, Skandalis SS, Gialeli C, Karamanos NK. Extracellular matrix structure. *Adv Drug Deliv Rev* 2016;97:4—27.
8. Petroll WM, Miron-Mendoza M. Mechanical interactions and crosstalk between corneal keratocytes and the extracellular matrix. *Exp Eye Res* 2015;133:49—57.
9. Ahmed M. Extracellular matrix regulation of stem cell behavior. *Curr Stem Cell Rep* 2016;2:197—206.
10. Choi JS, Kim EY, Kim MJ, et al. *In vitro* evaluation of the interactions between human corneal endothelial cells and extracellular matrix proteins. *Biomed Mater* 2013;8:014108.
11. Wilson SL, Wimpenny I, Ahearne M, Rauz S, Haj AJEl, Yang Y. Chemical and topographical effects on cell differentiation and matrix elasticity in a corneal stromal layer model. *Adv Funct Mater* 2012;22:3641—9.
12. Li Q, Wang H, Dai Z, Cao Y, Jin C. Preparation and biomechanical properties of an acellular porcine corneal stroma. *Cornea* 2017;36:1343—51.
13. Lee HI, Kim MK, Ko JH, Lee HJ, Lee JH, Wee WR. The characteristics of porcine cornea as a xenograft. *J Korean Ophthalmol Soc* 2006;47:2020—9.
14. Josifovska N, Niemi EM, Scholz H, Petrovski G. A pilot study for decellularizing human and porcine cornea for future use in corneal regeneration. *Acta Ophthalmol* 2024;102.
15. Guler S, Aslan B, Hosseinian P, Aydin HM. Supercritical carbon dioxide-assisted decellularization of aorta and cornea. *Tissue Eng C Methods* 2017;23:540—7.
16. Huang YH, Tseng FW, Chang WH, et al. Preparation of acellular scaffold for corneal tissue engineering by supercritical carbon dioxide extraction technology. *Acta Biomater* 2017;58:238—43.
17. Chaicharoenaudomrung N, Kunhorm P, Noisa P. Three-dimensional cell culture systems as an *in vitro* platform for cancer and stem cell modeling. *World J Stem Cell* 2019;11:1065—83.
18. Duval K, Grover H, Han LH, et al. Modeling physiological events in 2D vs. 3D cell culture. *Physiology* 2017;32:266—77.
19. Kim A, Zhou C, Lakshman N, Petroll WM. Corneal stromal cells use both high-and low-contractility migration mechanisms in 3-D collagen matrices. *Exp Cell Res* 2012;318:741—52.
20. Nishida K, Yamato M, Hayashida Y, et al. Corneal reconstruction with tissue-engineered cell sheets composed of autologous oral mucosal epithelium. *N Engl J Med* 2004;351:1187—96.
21. Bandeira F, Goh TW, Setiawan M, Yam GHF, Mehta JS. Cellular therapy of corneal epithelial defect by adipose mesenchymal stem cell-derived epithelial progenitors. *Stem Cell Res Ther* 2020;11:1—13.
22. Shangar S, Smith J, Allingham W, et al. Regeneration of corneal epithelium with dental pulp stem cells—an ex-vivo limbal stem cell deficiency model. *Investig Ophthalmol Vis Sci* 2020;61:1203.
23. Flaumenhaft R, Rifkin DB. Extracellular matrix regulation of growth factor and protease activity. *Curr Opin Cell Biol* 1991;3:817—23.
24. Petreaca M, Martins-Green M. Cell—extracellular matrix interactions in repair and regeneration. In: Atala A, Lanza R, Mikos AG, Nerem R, eds. *Principles of regenerative medicine*, 3rd ed. San Diego: Academic Press, 2019:15—35.
25. Rodrigues M, Griffith LG, Wells A. Growth factor regulation of proliferation and survival of multipotential stromal cells. *Stem Cell Res Ther* 2010;1:1—12.
26. Hu F, Wang X, Liang G, et al. Effects of epidermal growth factor and basic fibroblast growth factor on the proliferation and osteogenic and neural differentiation of adipose-derived stem cells. *Cell Reprogr* 2013;15:224—32.
27. Booth BW, Boulanger CA, Anderson LH, Jimenez-Rojo L, Brisken C, Smith GH. Amphiregulin mediates self-renewal in an immortal mammary epithelial cell line with stem cell characteristics. *Exp Cell Res* 2010;316:422—32.
28. Chen SQ, Cai Q, Shen YY, Cai XY, Lei HY. Combined use of NGF/BDNF/bFGF promotes proliferation and differentiation of neural stem cells *in vitro*. *Int J Dev Neurosci* 2014;38:74—8.
29. Wang X, Waldeck H, Kao WJ. The effects of TGF-α, IL-1β and PDGF on fibroblast adhesion to ECM-derived matrix and KGF gene expression. *Biomaterials* 2010;31:2542—8.
30. Toyoda S, Shin J, Fukuhara A, Otsuki M, Shimomura I. Transforming growth factor β1 signaling links extracellular matrix remodeling to intracellular lipogenesis upon physiological feeding events. *J Biol Chem* 2022;298:101748.
31. Chen YJ, Huang SM, Tai MC, Chen JT, Liang CM. Glucosamine impedes transforming growth factor β1-mediated corneal fibroblast differentiation by targeting Krüppel-like factor 4. *J Biomed Sci* 2019;26:72.
32. Donovan J, Shiwen X, Norman J, Abraham D. Platelet-derived growth factor alpha and beta receptors have overlapping functional activities towards fibroblasts. *Fibrogenesis Tissue Repair* 2013;6:10.
33. Marx M, Daniel TO, Kashgarian M, Madri JA. Spatial organization of the extracellular matrix modulates the expression of PDGF-receptor subunits in mesangial cells. *Kidney Int* 1993;43:1027—41.

34. Du Y, Roh DS, Funderburgh ML, et al. Adipose-derived stem cells differentiate to keratocytes *in vitro*. *Mol Vis* 2010;16: 2680—9.
35. Park SH, Kim KW, Chun YS, Kim JC. Human mesenchymal stem cells differentiate into keratocyte-like cells in keratocyte-conditioned medium. *Exp Eye Res* 2012;101:16—26.
36. Andresen JL, Ledet T, Ehlers N. Keratocyte migration and peptide growth factors: the effect of PDGF, bFGF, EGF, IGF-I, aFGF and TGF-beta on human keratocyte migration in a collagen gel. *Curr Eye Res* 1997;16:605—13.
37. Lin X, Wang H, Tan Y. Role of hepatocyte growth factor in wound repair. *Acta Acad Med Sin* 2018;40:822—6.
38. Shibuya M. Structure and function of VEGF/VEGF-receptor system involved in angiogenesis. *Cell Struct Funct* 2001;26:25—35.
39. Bach LA. Recent insights into the actions of IGFBP-6. *J Cell Commun Signal* 2015;9:189—200.